

Metasurface antennas embedded in small circular cavities for telemetry applications

L. Bernard, M. Martinis, Sylvain Collardey, K. Mahdjoubi, R. Sauleau

▶ **To cite this version:**

L. Bernard, M. Martinis, Sylvain Collardey, K. Mahdjoubi, R. Sauleau. Metasurface antennas embedded in small circular cavities for telemetry applications. Applied Sciences, 2019, 9 (12), pp.496. 10.3390/app9122496 . hal-02181457

HAL Id: hal-02181457

https://univ-rennes.hal.science/hal-02181457

Submitted on 7 Jul 2020

HAL is a multi-disciplinary open access archive for the deposit and dissemination of scientific research documents, whether they are published or not. The documents may come from teaching and research institutions in France or abroad, or from public or private research centers.

L'archive ouverte pluridisciplinaire **HAL**, est destinée au dépôt et à la diffusion de documents scientifiques de niveau recherche, publiés ou non, émanant des établissements d'enseignement et de recherche français ou étrangers, des laboratoires publics ou privés.

applied sciences

MDPI

Article

Metasurface Antennas Embedded in Small Circular Cavities for Telemetry Applications

Loïc Bernard [1,*], Mario Martinis [1,2], Sylvain Collardey [2], Kouroch Mahdjoubi [2] and Ronan Sauleau [2]

1 French-German Research Institute of Saint-Louis ISL, 68300 Saint-Louis, France
2 Univ Rennes, CNRS, IETR (Institut d'Electronique et de Télécommunications de Rennes)—UMR 6164, F-35000 Rennes, France; sylvain.collardey@univ-rennes1.fr (S.C.); ronan.sauleau@univ-rennes1.fr (R.S.)
* Correspondence: loic.bernard@isl.eu

Received: 24 April 2019; Accepted: 14 June 2019; Published: 19 June 2019



Featured Application: The small-cavity antennas introduced in this paper bring new capabilities to small flying platform instruments with telemetry capabilities.

Abstract: This paper introduces a metasurface-inspired antenna embedded in a circular metallic cavity with a very small diameter (from 0.25 λ_0 down to 0.12 λ_0, where λ_0 is the wavelength in vacuum at the operating frequency). The proposed concept is introduced and explained: It consists of placing a capacitive surface at the cavity aperture. This capacitive effect is obtained using multi-layer capacitively coupled strips. Our numerical results demonstrate that the impedance bandwidth is larger than that of standard patch antennas embedded in the same cavity size. Various prototypes have been manufactured, and measurements are found to be in good agreement with numerical results in all cases. The practical applications of these small metasurface antennas are demonstrated with telemetry applications for flying vehicles.

Keywords: circular cavities; metasurfaces; microstrip antennas; bandwidth

1. Introduction

Microstrip antennas are commonly used in modern wireless communications, as they present the advantages of low cost, low profile, and ease of fabrication, although they might suffer from a narrow bandwidth (BW) in certain configurations [1,2]. Furthermore, the integration of microstrip antennas into small cavities leads to antenna performance degradations. These have been investigated over the past decades in [3–6], and more recently in [7–9]. In particular, the reduction of the antenna diameter and its integration into a metallic cavity result in a significant decrease of its BW.

Furthermore, it was demonstrated in [7] that, for small cavities of rectangular shape (edge size of 0.25 λ_0, where λ_0 is the wavelength in vacuum at the operating frequency), a patch antenna placed at the aperture of the cavity does not offer the best performance in terms of BW: The maximum reachable BW was shown to be achieved by replacing a standard patch at the aperture with a metasurface composed of one or several layers of capacitively coupled strips [8], whose dimensions are typically smaller than one tenth of the wavelength [10]. As introduced in previous works [7–9,11], loading the aperture of a metallic cavity antenna with a capacitance-only impedance offers two benefits: Increasing the antenna BW [7], particularly compared to stacked patch antennas embedded in a larger cavity [11]; or reduction of the antenna and cavity size for a given BW [9].

Cavities of circular form are much more practical and common than rectangular ones. However, the integration of a metasurface antenna into a circular cavity is more difficult, because the field lines in rectangular cavities are parallel to the vertical wall, which is not the case for circular cavities, as will be

shown in the following sections. The novelty of the proposed work resides in two main aspects. First, our previous work on small rectangular cavity antennas [8] is extended here to the cases of circular cavities with a small diameter (0.25 λ_0), with the main objective to enlarge the antenna BW. Second, the metasurface antennas proposed here are integrated in very small cavities (0.15 λ_0 and 0.12 λ_0). In such cases, it is not possible to integrate standard patch antennas inside the cavity, provided that they are printed on dielectric substrates ($\varepsilon_r < 10.2$) that comply with the huge acceleration constraints and shocks imposed by the telemetry applications with flying vehicles we are considering here.

This paper is organized as follows: First, the concept of metasurface antennas in circular cavities is described in Section 2. The principle is explained, followed by a set of numerical results and the comparison with classical printed circular patches. Experimental results are presented. Section 3 deals with the analysis of metasurface antennas in smaller cavities optimized for integration on flying vehicles for telemetry applications. Conclusions are drawn in Section 4.

2. Circular Cavity Metasurface Antenna with a Diameter of 0.25 λ_0

2.1. Description of the Proposed Antenna

The metasurface cavity antenna, linearly polarized, is described in Figure 1. Its design fulfills the practical needs of manufacturing. Instead of a single circular patch, the metallization is divided into multiple metallic strips whose dimensions are much smaller than the wavelength (width < 0.1 λ_0). A design example with three strips is provided in Figure 1a. The shape of these strips is chosen to follow the E and H field lines of the TE_{11} mode excited inside the cavity, as illustrated in Figure 2. Such a shape allows for minimizing the disturbance of the field distribution at the aperture while effectively working as a distributed capacitance at the aperture. The gap g between the strips is adjusted to reach the right value of capacitance loading at the antenna aperture, as is the same for the rectangular case [8]. Increasing this gap g leads to a decrease of the capacitance value. This value is optimized in order to increase the bandwidth and keep the antenna well matched (reflection coefficient $|S_{11}| < -10$ dB). The substrate is bonded to the cavity wall using an organic glue ($\varepsilon_r = 3.5$ and $\tan\delta = 0.03$) whose thickness is labelled g_t. The glue degrades the antenna radiation performance, especially when the capacitance at the aperture is high. It is therefore desirable to make the gap g between the metasurface elements and the cavity wall as wide as possible, to keep the capacitance relatively low and to minimize the glue impact. In practice, g_t is set to 0.2 mm here. The aperture capacitance can be lowered by using a thin high-permittivity substrate on which the metasurface is etched, or it can be increased by using multiple layers, as shown in Figure 1b with two layers. The antenna is fed by a coaxial probe, and the outer conductor of the coaxial cable is soldered to a short tapered line to further enlarge the antenna BW (Figure 1b).

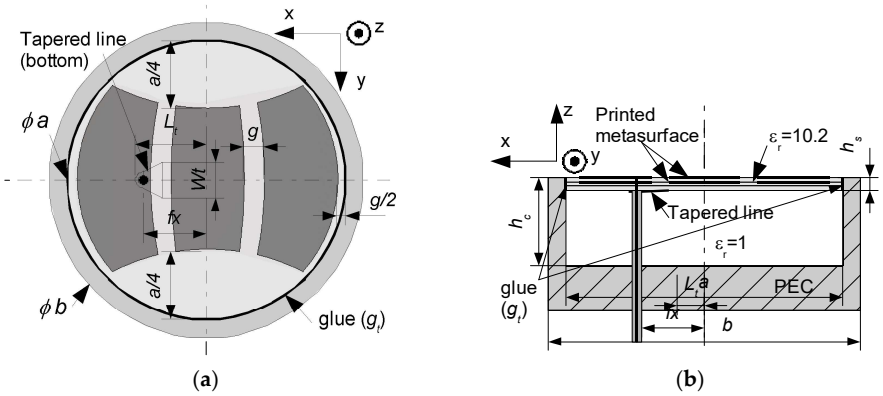


Figure 1. (**a**) Metasurface antenna with three strips at the aperture; and (**b**) cross-section view of the cavity showing the multilayer nature of the design.

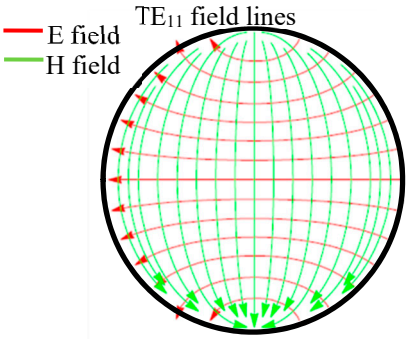


Figure 2. E and H fields of the TE_{11} cavity mode that served as inspiration for the metasurface shaping.

2.2. Description of the Reference Antenna: A Circular Patch Embedded in a Circular Cavity

The reference antenna structure is represented in Figure 3. It consists of a circular metallic cavity of external diameter b, inner diameter a, and height h_c. The cavity is entirely filled with a dielectric material of relative permittivity ε_r glued to the cavity bounds (no glue is considered in Section 2.4.: g_t = 0 mm, but g_t = 0.2 mm is realistic for practical cases). A circular patch of diameter d is printed on the upper face of the dielectric material. The patch is fed by a coaxial probe located at a distance f_x from the antenna center.

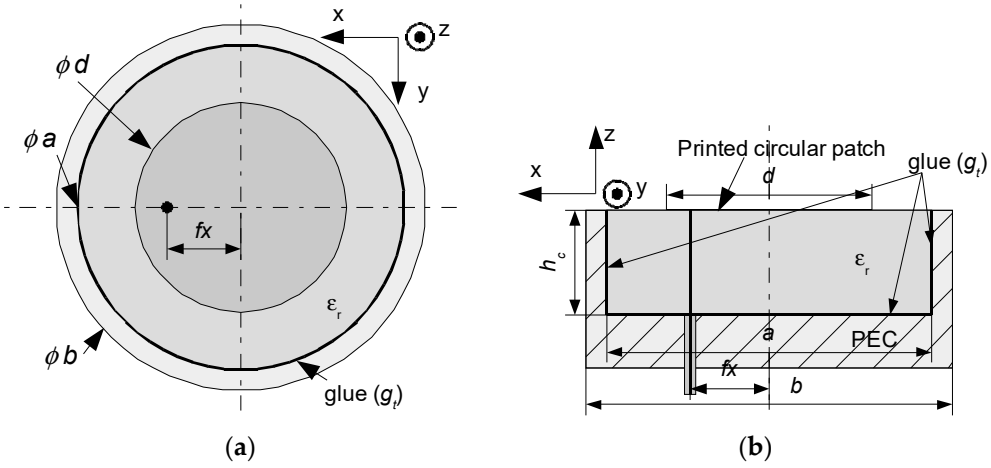


Figure 3. (**a**) Top view and (**b**) cross-section view of the reference circular antenna.

2.3. Simple Models for Describing Small-Cavity Antenna Bandwidth Behavior

2.3.1. Transmission Line Model of a Cavity Patch Antenna

A transmission line model of a small cavity with a patch has been introduced and analyzed in [12]. For consistency purposes, we briefly summarize the main conclusions of these findings. The cavity can be modeled as a short waveguide section, provided it is thick enough. If the waveguide is electrically short or under cutoff, the input admittance Y_{in}, seen from the aperture, is inductive. On the other hand, the aperture itself is modeled by an aperture admittance $Y_{Ap} = G_{Ap} + jB_{Ap}$, where G_{Ap} represents radiation conductance and B_{Ap} is the susceptance modeling the near field which, for a small aperture, is also inductive (as a result of high currents on cavity walls). For a finite outer diameter of the cavity, Y_{Ap} has to be obtained numerically [12]. The patch antenna placed at the aperture allows for the structure to be brought into resonance. The patch presents a high capacitance C_P (from patch edge to cavity wall). However, modeling the patch only as a capacitance is not realistic, due to the current

flowing on its surface. The effect of this current is modeled for by adding an inductance L_P in series with C_P. Figure 4 shows the proposed model, for which the resonance condition can be written as:

$$jY_{Ap} - j\frac{k_{TE}}{k\,\eta_0}\cot(k_{TE}h_c) + \frac{1}{\frac{1}{j\omega C_P} + j\omega L_P} = 0 \quad (1)$$

where $k_{TE}^2 = \varepsilon_r k^2 - k_c^2$, $k^2 = \omega^2\mu_0\epsilon_0, k_c = p'_{11}/r$, and h_c is the cavity height (r is the aperture radius and p'_{11} is the first zero of $J'_1(k_c r)$).

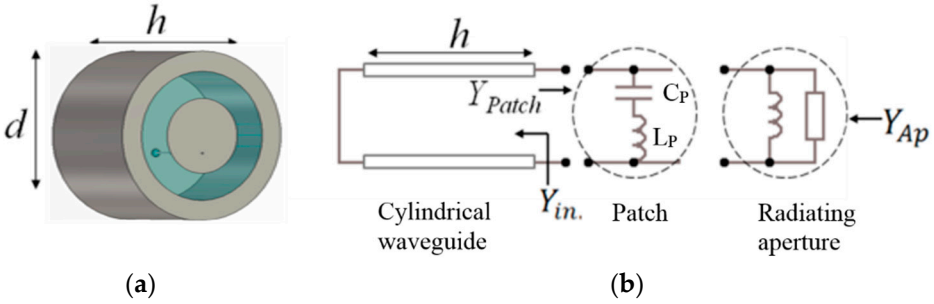


Figure 4. (**a**) Patch at the aperture of the cavity; and (**b**) electrical model of the patch in the cavity.

This model [12] was shown to give a qualitative explanation of the bandwidth behavior for patch antennas in cavities. One important prediction is that the cavity volume needs to be filled with $\varepsilon_r \gg 1$ for an enlarged BW. For low permittivity (for example air), the patch would need to cover almost the entire aperture area, leading to a very tiny gap with the cavity wall and thus causing manufacturing and BW issues [12].

2.3.2. Transmission Line Model of a Cavity Metasurface

Figure 5 represents the model for a cavity with a metasurface at the aperture. This is essentially the same as the model analyzed in [8]. Arranging multiple smaller patches instead of a single large patch leads to a decrease of the series "patch inductance", and gives the desired result of only a capacitance C_{eq} at the aperture. This leads to a smaller Q factor (less energy storage), and hence an increase in BW. By splitting the patch and reducing the sizes of the metallic strips, we are essentially "cutting" the current that usually exists in the center of a patch surface into smaller pieces, which reduces the inductive effect.

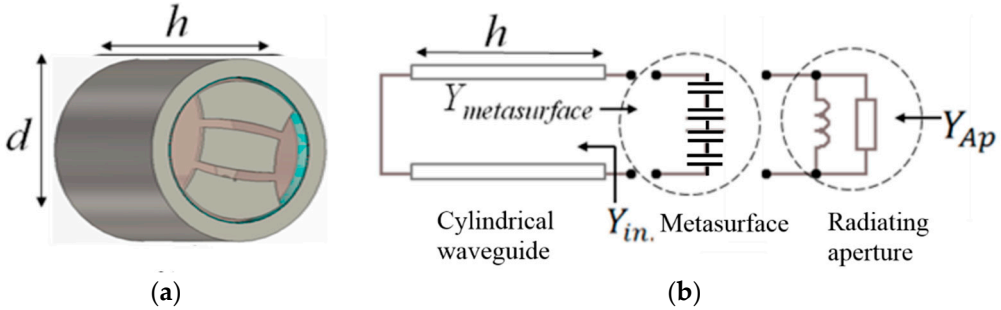


Figure 5. (**a**) Cavity antenna with parasitic capacitance (realized by a metasurface) at the aperture, and (**b**) its electrical model.

The resonance condition from this model is given by:

$$jY_{Ap} - j\frac{k_{TE}}{k\,\eta_0}\cot(k_{TE}h_c) + j\omega C_{eq} = 0. \quad (2)$$

Once the resonance condition (2) is satisfied, for a set $\left(h_c,\ C_{eq}\right)$, if ε_r is taken to be 1 (which turns out to be the best case for BW), one can calculate the Q factor of such an antenna using:

$$Q_{Ant.} = \frac{\omega_0}{2\, G_{Ap}(\omega_0)} \left| \frac{\partial Y(\omega_0)}{\partial \omega} \right| \tag{3}$$

where Y is the sum of the aperture and waveguide admittances, and the derivative is evaluated at the resonance frequency ω_0. From the Q factor, $S_{11} < -10$ dB, and fractional bandwidth is given by $FBW = 2/3Q$.

2.4. Bandwidth Performance of Small Circular Cavity Antennas

The transmission line (TL) models given above are very attractive to provide a qualitative explanation of the BW behaviors of patch antennas and metasurface antennas in cavities. As demonstrated in [8], the inductance is the blocking point, which does not permit the antennas to achieve the maximum achievable BW (according to the predictions based on Gustafsson's bound [8,13]). Nevertheless, this upper limit can be reached using a structure having parasitic capacitance only (instead of the patch). Moreover, it was demonstrated in [8] that the Q factor and BW predicted by the TL model are in good agreement with theoretical values for minimum Q (maximum BW), as shown in [13]. Hence, we concentrate here only on the predicted values of Q and BW using the TL model.

These numerical results, obtained with the TL model and full-wave electromagnetic simulations using the commercial software CST Microwave Studio [14], are plotted in Figure 5 for a metasurface antenna design with a cavity diameter a = 32 mm ($0.25\lambda_0$). The center frequency is chosen to be 2300 MHz (λ_0 = 130 mm).

Figure 6 shows that, for the considered cavity diameter a, the BW increases with the cavity height h_c up to a given value, after which it stays quasi-constant. These theoretical results have been validated by full-wave simulations of metasurfaces using the CST software [14]. The maximum achievable BW is 77 MHz for h_c = 20.0 mm. Nevertheless, for a smaller value of h_c (15.0 mm), the BW (75 MHz) is quite close to this maximum. It is to be noted that these simulations are carried out considering ideal materials without any losses ($g_t = 0$) in order to compare the full-wave results to the ones from the TL models, and also to assess the theoretical maximum achievable BW induced by the cavity resonance. In practice, losses would result in widening the BW but decreasing the antenna efficiency.

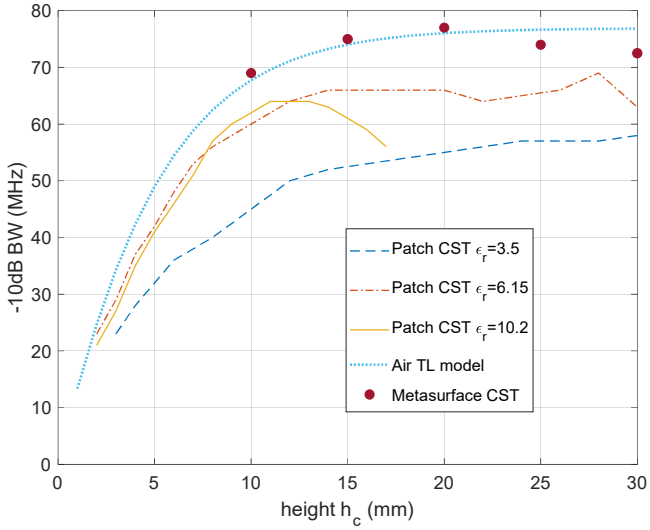


Figure 6. Maximum achievable bandwidth (BW) calculated with the transmission line (TL) model and simulated BW (with CST software) for three reference patches (with three different dielectric substrates) and for a metasurface within cavities of diameter a = 32 mm (no glue). The solid blue line displays the maximum achievable BW computed with the TL model [8,12,13].

For comparison purposes, the BW of standard circular patch antennas (Figure 3) embedded in a circular cavity of the same diameter (a = 32 mm) has been also reported in Figure 6 for three permittivity values. These results have been obtained using CST Microwave Studio [14], and no glue is considered. Comparison between the results plotted in Figure 6 shows that the BW achieved with patch antennas is narrower than with metasurfaces: 64 MHz for reference patches printed on ε_r = 6.15 (h_c = 12.0 mm) or on ε_r = 10.2 (h_c = 12.0 mm), compared to 77 MHz (h_c = 20.0 mm) or 75 MHz (h_c = 15.0 mm) for the metasurface. Furthermore, it has to be noted that for the patch case, the maximum of BW is not achieved with the lowest permittivity material, and even that the BW is similar for ε_r = 6.15 and ε_r = 10.2 for a thickness of h_c = 12.0 mm. Increasing the thickness further does not result in significantly enlarging the BW.

To be more exhaustive in the comparison, a patch antenna in a cavity of diameter a = 32 mm and thickness h_c = 12.0 mm was also considered on a dual-layer substrate: 10.1 mm of air (ε_r = 1) and 1.9 mm of RO3010 (ε_r = 10.2), as is the case for the metasurface. The cross-section view is given in Figure 7. After optimization, the BW was 65 MHz, demonstrating that the achievable BW with a patch is narrower than with the metasurface in a small cavity. The above conclusions are in agreement with the one derived for rectangular cavities [8,12].

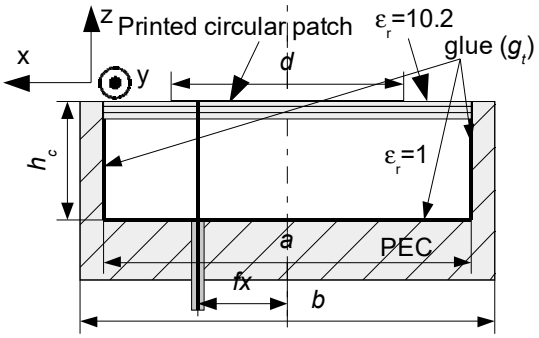


Figure 7. Cross-section view of the circular patch antenna on dual-layer substrate.

2.5. Experimental Results

A prototype of a metasurface antenna in a cavity of diameter 0.25 λ_0 has been manufactured. The cavity inner diameter is a = 32 mm (0.25 λ_0) and the outer one equals b = 42 mm. The cavity height is chosen from the above simulation results, and corresponds to the maximum or nearly maximum BW: h_c = 15.0 mm. All dimensions have been optimized using CST Microwave Studio [14] in order to minimize the reflection coefficient at 2300 MHz. As per design guidelines, the parameter g is first optimized to tune the frequency (increasing g increases the frequency). The value of f_x is chosen to ensure that the feeding point lies on the left strip (and not on its edge). Secondly, the parameters L_t and W_t are optimized to minimize the reflection coefficient and to finely tune the frequency. The final parameters are provided in Table 1. A photograph of the prototype is given in Figure 8: The feeding point is visible on the bottom strip, whereas a second hole can be seen on the top strip. These two centering holes are used to align the three printed layers during the assembly process. After this step, the coaxial cable is soldered to the top metasurface and to the tapered line at the bottom of the stack up. The proposed antenna presents a total thickness of 1.92 mm, and is glued into the cavity. The metallization forming the metasurface has a gap g = 2.3 mm. The other dimensions can be found in Table 1. The cavity below the dielectric layers is kept free of material, i.e., with a relative permittivity of ε_r = 1.

Simulation results (including losses) are given in Figure 9. The antenna BW equals 82 MHz. The measurement results are in close agreement with the simulations, having a slightly larger BW of 90 MHz. This BW enlargement might come from a possible undervaluation of the insertion due to the glue. Moreover, a second resonance can be observed in measurement, which also contributes to the BW enlargement. The measured gain is of 3.9 dBi (simulated gain is 4.5 dBi). The measured

antenna efficiency equals 79.4%. The measured radiation patterns are provided in Figure 10, with a cross-polarization discrimination (XPD) of 21.9 dB. The main radiation characteristics are summarized in Table 1 (the term HPBW stands for Half Power Beamwidth).

Table 1. Prototype dimensions and performances for a cavity of 32 mm.

Substrate	RO3010 +air	Sim. BW (MHz)	82
a (mm)	32.0	Meas. BW (MHz)	90
Dielectric layers (mm)	3×0.63	Sim. gain (dB)	4.5
h_c (mm)	15	Meas. gain (dB)	3.9
f_x (mm)	6.6	Meas. efficiency (%)	79.4
g (mm)	2.3	Meas. XPD (dB)	21.9
L_l (mm)	5.14	Meas. HPBW E-plane (°)	95
W_l (mm)	4.8	Meas. HPBW H-plane (°)	81



Figure 8. Photograph of the metasurface prototype within a cavity of 32 mm (0.25 λ_0, where λ_0 is the wavelength in vacuum at the operating frequency).

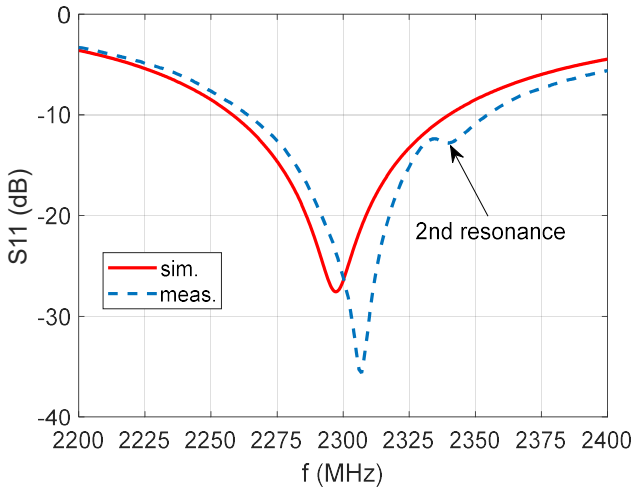
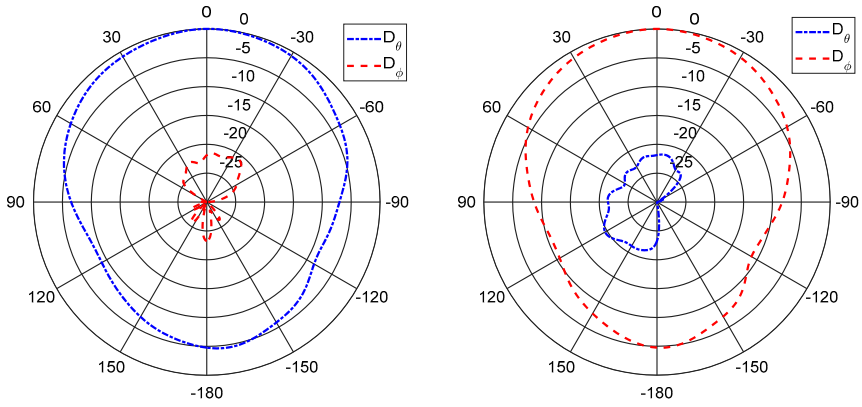


Figure 9. Simulated and measured reflection coefficients for the metasurface antenna in a cavity of diameter 0.25 λ_0.



(**a**) E-plane (**b**) H-plane

Figure 10. Measured radiation patterns at f = 2310 MHz in the E- and H-planes of the metasurface antenna in a cavity of diameter 0.25 λ_0.

3. Metasurface Antennas in Small Cavities for Telemetry Applications

Very small cavity sizes are considered here, namely of 20 and 16 mm. They are intended to be integrated into small flying vehicles, and therefore must be extremely mechanically robust to support shocks and high accelerations.

3.1. Cavity Diameter of 0.15 λ_0

3.1.1. Patch with Cavity Diameter a = 20 mm (0.15 λ_0)

Although an ideal simulation of a patch antenna within a cavity of diameter 20 mm can give good matching at 2.3 GHz (h_c = 14 mm, d = 18.38 mm, f_x = 2.8 mm), the realistic simulation, taking into consideration a glue layer of thickness 0.2 mm, showed that the resonance frequency shifts to a higher frequency and cannot be shifted back by increasing the patch size. With a diameter a = 20 mm, the realization of a patch antenna printed on RO3010 substrate is not feasible with the manufacturing process we use.

3.1.2. Metasurface with Cavity Diameter a = 20 mm (0.15 λ_0)

The antenna structure is represented in Figure 11. The cavity thickness is h_c = 14 mm, and the optimized dimensions are given in Table 2. The external diameter of the cavity is 28 mm. Five layers of RO3010 are glued together, and four layers of metasurfaces are printed on the four upper ones. The rest of the volume is filled with Polypropylene (PP, ε_r = 2.26 and δ = 0.002 [15]), instead of air, to enhance its mechanical resistance.

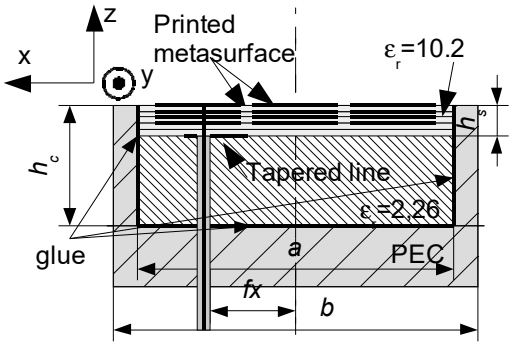


Figure 11. Side view of the cavity, showing a multilayer design of diameter 20 mm.

Table 2. Prototype dimensions and performances for a cavity of 20 mm.

Substrate	RO3010 +PP	Sim. BW (MHz)	20
a (mm)	20.0	Meas. BW (MHz)	21
Dielectric layers (mm)	5 × 0.63	Sim. gain (dB)	0.8
h_c (mm)	14	Meas. gain (dB)	−1.0
f_x (mm)	4.1	Meas. efficiency (%)	37.7
g (mm)	1.68	Meas. XPD (dB)	28.0
L_l (mm)	1.45	Meas. HPBW E-plane (°)	158
W_l (mm)	4.8	Meas. HPBW H-plane (°)	102

The manufactured antenna is well matched and resonates close to 2.3 GHz (Figure 12), as predicted by the simulation. The measured BW is 21 MHz, which is in good agreement with simulation results, but the measured gain is lower than the simulated one (−1 dBi in experiment versus 0.8 dBi in simulation), indicating slightly higher loss due to the glue. The radiation characteristics are given in Table 2, and measured radiation patterns are represented in Figure 13. The beam is wider than for a diameter of 32 mm, especially in the E-plane (HPBW of 158°). The measured antenna efficiency is 37.7%. This drop is explained by the small size of the antenna (0.15 λ_0) in comparison to the previous antenna (0.25 λ_0). Indeed, the radiation efficiency of the small antenna is related to its volume (the sphere in which the antenna fits), and it decreases with the reduction of this volume [16,17].

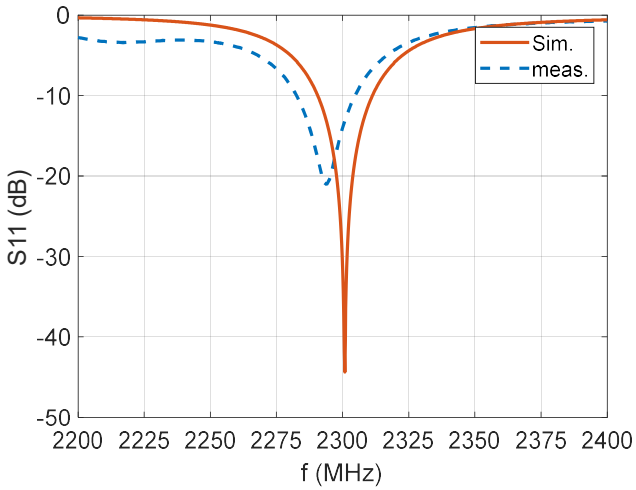


Figure 12. Simulated and measured reflection coefficients for the metasurface antenna in a cavity of diameter 0.15 λ_0.

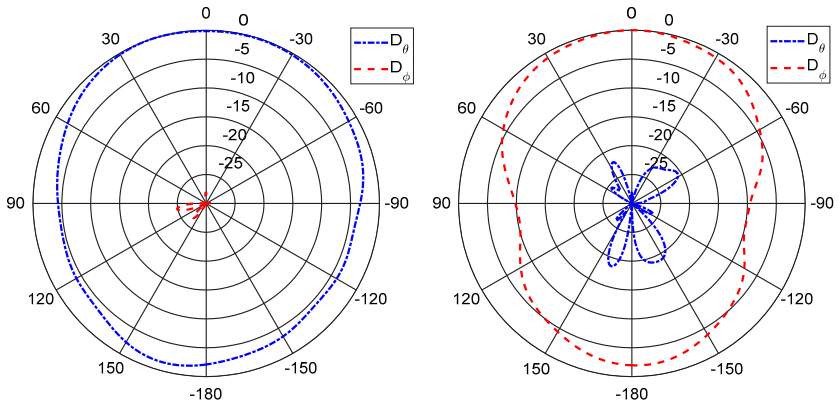


Figure 13. Measured radiation patterns in the E- and H-planes of the metasurface antenna in a cavity of diameter a = 20 mm, at the frequency of f = 2290 MHz.

3.2. Cavity Diameter of 0.12 λ_0

3.2.1. Validation Design with h_c = 14 mm

Six layers of RO3010 are used at the aperture of the cavity, and the total cavity thickness is h_c = 14 mm. The metasurface is composed of only two strips which are much smaller than the wavelength, as described in Figure 14. The dimensions are given in Table 3. The external diameter of the cavity is 20 mm. Measured results (given in Figure 15) show that the manufactured antenna resonance is shifted to 2.37 GHz. This shift (3%) could be attributed to the characteristics of the glue, which are not well known in this frequency range, and to its strong influence on the resonance conditions with such small dimensions. The BW is similar to the simulated value, but the gain is reduced (−5.5 dBi versus −3.0 dBi), indicating extra losses in experiments. Again, the main cause of the loss increase is believed to be the glue. The cross-polarization level is very low (−32.5 dB) and the beam is wide due to the small diameter, especially in the E-plane (see Figure 16). The measured antenna efficiency is 13.5%—this value is physically limited by the small volume of this antenna [16,17].

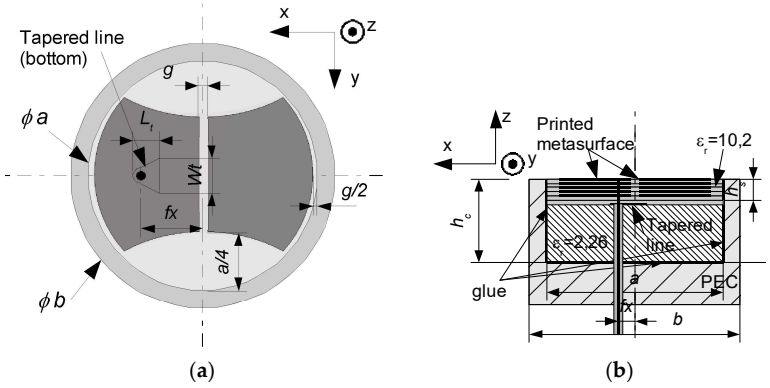


Figure 14. (**a**) Metasurface of two strips at the aperture, and (**b**) side view of the cavity showing a multilayer design of diameter 16 mm.

Table 3. Prototype dimensions and performances for a cavity of 16 mm and a thickness of 14 mm.

Substrate	RO3010 +PP	Sim. BW (MHz)	20
a (mm)	16.0	Meas. BW (MHz)	20
Dielectric layers (mm)	6 × 0.63	Sim. gain (dB)	−3.0
h_c (mm)	14	Meas. gain (dB)	−5.5
f_x (mm)	0.6	Meas. efficiency (%)	13.5
g (mm)	1.37	Meas. XPD (dB)	32.5
L_l (mm)	1.43	Meas. HPBW E-plane (°)	/
W_l (mm)	4.0	Meas. HPBW H-plane (°)	93

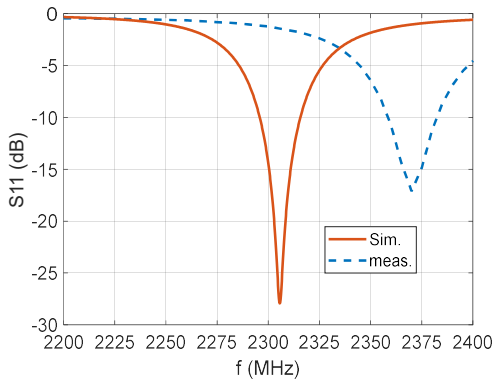


Figure 15. Simulated and measured reflection coefficients for the metasurface antenna in a cavity of diameter 0.12 λ_0.

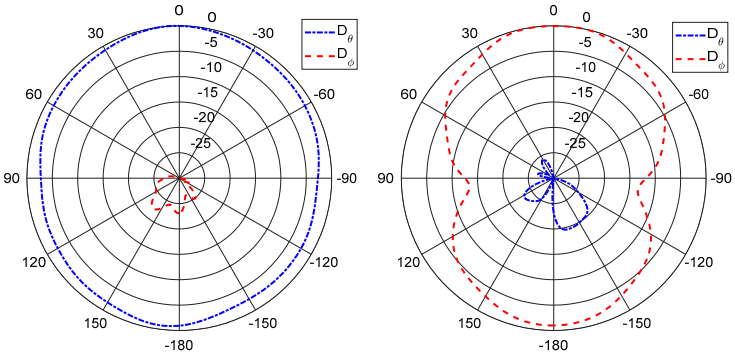


Figure 16. Measured radiation patterns in the E- and H-planes of the metasurface antenna for a cavity diameter of a = 16 mm, at the frequency of f = 2370 MHz.

3.2.2. Design for Projectiles with h_c = 12.6 mm

With the objective to integrate a telemetry unit onboard two types of gun-launched projectiles of caliber 24 mm, an upgrade of the metasurface antenna presented above is proposed here in order to further reduce its thickness down to h_c = 12.6 mm. The first one is illustrated in Figure 17a, and is an innovative concept of a Long Range Projectile with large wings [18,19]. The second one is a gyrostabilized projectile, which can be seen in Figure 17b. Its profile is described as Secant Ogival Cylinder Boat Tail (SOCBT) [20]. For these two projectiles, the antenna should be integrated in the rear part, within a reduced section, as can be seen in Figure 17. A protective layer has been added on the top of the metasurface antenna to protect it from potential powder deposits and from flames during the firing.



(**a**)



(**b**)

Figure 17. Instrumented projectiles: (**a**) Long Range Projectile of caliber 24 mm and (**b**) Secant Ogival Cylinder Boat Tail (SOCBT) of caliber 30 mm.

The optimization of this new design was partially presented in [21]. The cavity diameter is a = 16 mm and its thickness is h_c = 12.6 mm. The PP block at the bottom is 7.7 mm high. Six layers of metasurface are stacked, requiring seven layers of RO3010 material, each with a thickness of 0.63 mm. Their shape is constituted of two parts, as shown in Figure 14a. On the top of this stack up, a thin layer

of RO4350 (of thickness 0.5 mm and of permittivity $\varepsilon_r = 3.5$) is glued. The optimized dimensions are given in Table 4. The matching level and resonance frequency are tuned using three main parameters, namely g, L_t, and W_t, and their respective influences are described in [21]. In this set up, g has a strong influence on the resonance frequency, whereas L_t and W_t are mostly used to match the antenna.

Table 4. Prototype dimensions and performances for a cavity of 16 mm and a thickness of 12.6 mm.

Substrate	RO4350+ RO3010 +PP	Sim. BW (MHz)	15
a (mm)	16.0	Meas. BW (MHz)	20
Dielectric layers (mm)	$1 \times 0.5 + 7 \times 0.63$	Sim. gain (dB)	−3.0
h_c (mm)	12.6	Meas. gain (dB)	−5.5
f_x (mm)	1.4	Meas. efficiency (%)	14.5
g (mm)	0.3	Meas. XPD (dB)	33.5
L_l (mm)	4.2	Meas. HPBW E-plane (°)	126
W_l (mm)	4.0	Meas. HPBW H-plane (°)	97

The measured radiation patterns are given in Figure 18, whereas the overall performance is summarized in Table 4. It should be noted that due to the projectile body, the radiation patterns are slightly more directive than for the antenna of diameter 16 mm alone (see Figure 16).

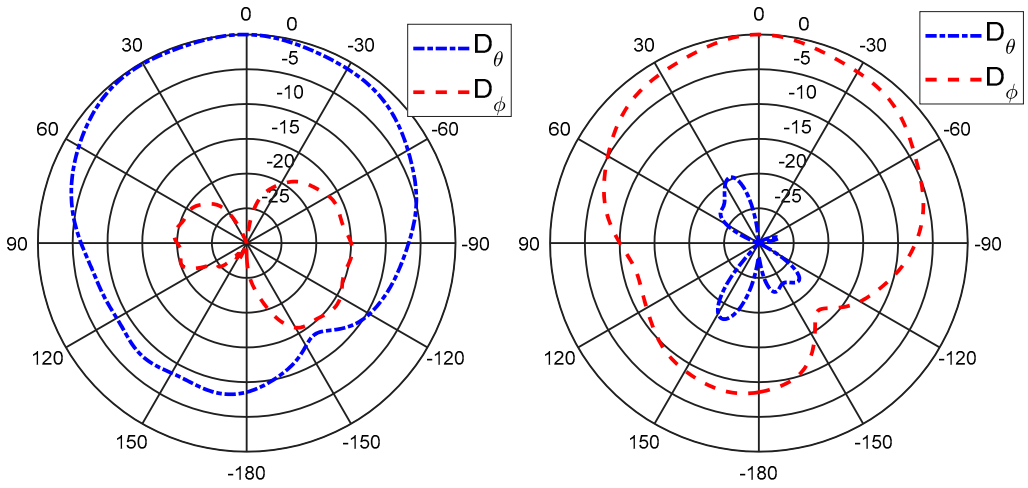


Figure 18. Measured radiation patterns in the E- and H-planes of the metasurface antenna for the projectile SOCBT, at the frequency of f = 2290 MHz.

These small antennas have been successfully tested at ISL, France, during measurement campaigns for both projectile types under accelerations of up to 25,000 g and a spin rate of about 300 Hz [19].

4. Conclusions

Metasurface-inspired antennas have been proposed to enlarge the bandwidth of small antennas embedded in miniature circular cavities. The design is inspired from the distribution of the E and H fields of cavity mode TE_{11}, and the principle is based on imposing a capacitive-only impedance at the aperture of the cavity to enlarge the antenna bandwidth. We demonstrated numerically and experimentally that these structures exhibit a larger bandwidth and efficiency compared to conventional cavity patch antennas, without degrading their radiation characteristics. Moreover, we also showed that the proposed concepts can also be applied to very small cavity diameters (0.15 λ_0 and 0.12 λ_0), in which standard patch antennas cannot be integrated due to their too-large size. These innovative small cavity antennas bring new opportunities for the instrumentation of smaller carriers and have been successfully tested for telemetry applications in harsh environments.

Author Contributions: All authors contributed to all tasks, but below are mentioned the main contributors for each tasks. Concept and design: M.M. and K.M.; Simulations and experiments: M.M., S.C. and L.B.; Draft Preparation: L.B., M.M., S.C., K.M. and R.S.; Review: L.B., S.C. and R.S.; Supervision: K.M. and R.S.

Funding: This research was partially funded by the Région Bretagne ARED program, and the French–German Research Institute of Saint-Louis.

Conflicts of Interest: The authors declare no conflict of interest.

References

1. Pozar, D.M. Microstrip antennas. *Proc. IEEE* **1992**, *80*, 79–91. [CrossRef]
2. Bahl, I.J.; Bhartia, P. *Microstrip Antennas*; Artech House: Norwood, MA, USA, 1980.
3. Karmakar, N.C. On miniaturisation and bandwidth enhancement of a cavity backed circular microstrip patch antenna. In Proceedings of the IEEE Antennas and Propagation Society International Symposium, San Antonio, TX, USA, 16–21 June 2002; Volume 3, pp. 596–599.
4. Karmakar, N.C. Investigations into a cavity-backed circular-patch antenna. *IEEE Trans. Antennas Propag.* **2002**, *50*, 1706–1715. [CrossRef]
5. Aberle, J.T. On the use of metallized cavities backing microstrip antennas. In Proceedings of the Antennas and Propagation Society Symposium, London, ON, Canada, 24–28 June 1991; Volume 1, pp. 60–63.
6. Zavosh, F.; Aberle, J.T. Improving the performance of microstrip patch antennas. *IEEE Antennas Propag. Mag.* **1996**, *38*, 7–12. [CrossRef]
7. Martinis, M.; Mahdjoubi, K.; Sauleau, R.; Collardey, S.; Bernard, L.; Valerio, G. On maximum bandwidth of rectangular cavity antennas with broadside radiation pattern. *IEEE Antennas Wirel. Propag. Lett.* **2014**, *13*, 1709–1712. [CrossRef]
8. Martinis, M.; Mahdjoubi, K.; Sauleau, R.; Collardey, S.; Bernard, L. Bandwidth behavior and improvement of miniature cavity antennas with broadside radiation pattern using a metasurface. *IEEE Trans. Antennas Propag.* **2015**, *63*, 1899–1908. [CrossRef]
9. Martinis, M. Development and Characterization of Metamaterials in Cavities. Applications to the Design of Compact Antennas. Ph.D. Thesis, University of Rennes 1, Rennes, France, November 2014.
10. Faenzi, M.; Minatti, G.; Maci, S. Metasurface antennas: Design and performance. *IEICE Trans. Commun.* **2019**, *E102-B*, 174–181. [CrossRef]
11. Martinis, M.; Bernard, L.; Mahdjoubi, K.; Sauleau, R.; Collardey, S. Wideband antenna in cavity based on metasurfaces. *IEEE Antennas Wirel. Propag. Lett.* **2016**, *15*, 1053–1056. [CrossRef]
12. Martinis, M.; Mahdjoubi, K.; Sauleau, R.; Collardey, S.; Bernard, L. Circuit models explaining bandwidth behavior of small circular cavity backed patch antennas. In Proceedings of the 8th European Conference on Antennas and Propagation (EuCAP 2014), The Hague, The Netherlands, 6–11 April 2014; pp. 3652–3656.
13. Gustafsson, M.; Sohl, C.; Kristensson, G. Physical limitations on antennas of arbitrary shape. *Proc. R. Soc. A* **2007**, *463*, 2589–2607. [CrossRef]
14. CST Studio Suite. Available online: https://www.3ds.com/products-services/simulia/products/cst-studio-suite/ (accessed on 18 June 2019).
15. Cos, M.E.; Las-Heras, F. Polypropylene-based dual band CPW-fed monopole antenna. *IEEE Antennas Propag. Mag.* **2013**, *55*, 264–273. [CrossRef]
16. Best, S.R. Low Q electrically small linear and elliptical polarized spherical dipole antennas. *IEEE Trans. Antennas Propag.* **2005**, *53*, 1047–1053. [CrossRef]
17. Sarrazin, F.; Pflaum, S.; Delaveaud, C. Radiation efficiency improvement of a balanced miniature IFA-inspired circular antenna. *IEEE Antennas Wirel. Propag. Lett.* **2017**, *16*, 1309–1312. [CrossRef]
18. Albisser, M.; Dobre, S.; Decrocq, C.; Saada, F.; Martinez, B.; Gnemmi, P. Aerodynamic Characterization of a new concept of long range projectiles from free-flight data. In Proceedings of the 30th International Symposium on Ballistics (ISB), Long Beach, CA, USA, 11–15 September 2017.
19. Saada, F.; Zeiner, A.; Meder, K.; Garcia-Gamez, L.; Bernard, L. Miniaturized onboard electronics for attitude measurement of medium caliber projectiles. In Proceedings of the IEEE International Conference on Electronics Circuits and Systems (ICECS), Bordeaux, France, 9–12 December 2018.

20. Albisser, M.; Saada, F.; Bernard, L.; Adam, R.; Zeiner, A. Design optimization of an instrumented spin-stabilized projectile developed for the aerodynamic characterization from free flight data. In Proceedings of the International Symposium of Ballistic 2019, Hyderabad, India, 4–8 November 2019.
21. Gámez, L.G.; Martinis, M.; Bernard, L.; Sauleau, R.; Collardey, S.; Mahdjoubi, K.; Pouliguen, P.; Potier, P. Antenne miniature en cavité circulaire à base de métasurfaces. In Proceedings of the Journées Nationales Micro-ondes (JNM), St Malo, France, 16–19 May 2017.



© 2019 by the authors. Licensee MDPI, Basel, Switzerland. This article is an open access article distributed under the terms and conditions of the Creative Commons Attribution (CC BY) license (http://creativecommons.org/licenses/by/4.0/).